


SCIENTIFIC REPORTS



OPEN

A necessary criterion for obtaining accurate lattice parameters by Rietveld method

Masami Tsubota¹ & Jiro Kitagawa² 

To obtain the lattice parameters accurately by the Rietveld method, the relationship between the lattice parameters and the peak-shift, which is the deviation in diffraction angle from the theoretical Bragg position, was studied. We show that the fitting accuracy of lattice parameters is related directly to the well reproducibility of the peak-shift. This study unveils that the peak-shift consists of the experimental and the analytical ones. The analytical peak-shift erroneously lowers a reliability factor R_{wp} , which has, so far, been the conventional criterion of fit. The conventional Rietveld method obtains a unit-cell which is a homothetic (proportional) unit-cell of the true one. We propose an additional criterion based on the peak-shift to obtain the true lattice parameters accurately. Our criterion can achieve reproducibility reasonably well for the experimental peak-shift, leading to highly improved accuracy of the lattice parameters.

Structural study for powder materials relies on the Rietveld method, which is capable of refining the structural and magnetic parameters from diffraction data^{1–3}. However, it is fundamentally difficult to determine accurately the refinement parameters^{4–7}. In the Rietveld method, the weighted sum of squares residual, S_p , between the observed and the calculated intensities of powder diffraction data is minimized in a nonlinear least-squares method. The calculated intensity includes the peak-shift that is absolutely inevitable in the experiment. To evaluate quantitatively the best fit of the data, several reliability-factors such as R_{wp} , R_p , R_e , R_f , S and χ^2 are proposed^{3,4}. The most accepted factor is the weighted-profile R , termed as R_{wp} , where the numerator includes S_r that is minimized during the refinements. The goodness-of-fit, S or $\chi^2 \equiv S^2$, is used as another useful numerical criterion⁴. The S -value of 1.3 or less is empirically considered to be satisfactory. However, a poor counting statistics or a high background also makes S smaller; the S -value sometimes turns out to be less than 1.0. On the other hand, S may possibly be larger than 1.3 even for the best fitting with an appropriate model. Young and co-workers have suggested that these values to be given in publication⁸.

Strictly speaking, there is no general agreement on these criteria in the Rietveld method. Other studies have concluded that viewing the profile-plots is more effective than R -values to determine the quality of a refinement^{5–7}. As such, the refined structural parameters have been found to differ from researcher to researcher. For instance, Hill summarized the results of Rietveld refinements on the project undertaken by the Commission on Powder Diffraction of the International Union of Crystallography⁷. Several specialists analysed the *standard* PbSO_4 powder diffraction pattern, measured by a conventional Bragg–Brentano diffractometer using $\text{Cu K}\alpha$ radiation. The lattice parameters a , b and c are in the range of 8.4764–8.4859 Å, 5.3962–5.4024 Å and 6.9568–6.9650 Å, respectively. The accuracy of the lattice parameters is of an order of 0.01 Å ($=10 \times 10^{-3}$ Å), which is incomparably large considering that the linear thermal expansion coefficient is of an order of 10^{-5} K⁻¹ to 10^{-6} K⁻¹ for general solid materials⁹. Furthermore, the weighted mean parameters for a -, b - and c -axes are 8.4804(4) Å, 5.3989(3) Å and 6.9605(2) Å, respectively. They are in good agreement with those determined from single-crystal X-ray diffraction data^{7,10} which is generally accepted to be high-accuracy. These facts mean that either smaller or larger lattice parameter compared to the true one is possibly obtained depending on a researcher by the Rietveld method. This is a critical disadvantage to study the dependences of lattice parameters on temperature, composition, pressure and so on. A technique to determine refinement parameters accurately is needed for the Rietveld method.

¹Physonit Inc., 6-10 Minami-horikawa, Kaita, Aki, Hiroshima, 736-0044, Japan. ²Department of Electrical Engineering, Faculty of Engineering, Fukuoka Institute of Technology, 3-30-1 Wajiro-higashi, Higashi-ku, Fukuoka, 811-0295, Japan. Correspondence and requests for materials should be addressed to M.T. (email: tsubota@physonit.jp)

We shed light on the peak-shift that tends to be overlooked. This paper proposes an additional criterion, focusing on a fitting accuracy along the horizontal-axis of powder diffraction data, to determine the lattice parameters accurately. In the following, we demonstrate that our criterion enables the well reproducibility of the peak-shift, leading to highly improved accuracy of the lattice parameter by two or more digits lower compared to that obtained by the conventional Rietveld method.

The X-ray diffraction pattern of standard reference material (SRM) 660a (lanthanum hexaboride)¹¹ from the National Institute of Standards and Technology (NIST) collected with Cu $K\alpha_1$ radiation was used in this study. We focused on the maximum diffraction angle ($2\theta_{\max}$) of the data used in the analysis. We conducted several conventional Rietveld refinements in the 2θ -range from 18° to $2\theta_{\max}$, where $2\theta_{\max}$ was in between 52° and 152° . There were five Bragg-peaks for $2\theta_{\max} = 52^\circ$ and twenty-four Bragg-peaks for $2\theta_{\max} = 152^\circ$. The representative results for $2\theta_{\max} = 152^\circ$ and 92° are demonstrated.

Results

Rietveld refinements. In the conventional Rietveld refinement, the lattice parameters are $a^{\text{cnv},(152)} = 4.15655(1) \text{ \AA}$ with $R_{\text{wp}}^{\text{cnv},(152)} = 8.203\%$ and $a^{\text{cnv},(92)} = 4.15811(22) \text{ \AA}$ with $R_{\text{wp}}^{\text{cnv},(92)} = 8.610\%$, where the superscripts ‘cnv’, (152) and (92) refer to the ‘conventional’, $2\theta_{\max} = 152^\circ$ and 92° , respectively. Here, $a^{\text{cnv},(152)}$ and $a^{\text{cnv},(92)}$ are $0.37 \times 10^{-3} \text{ \AA}$ (or 0.0089%) smaller and $1.19 \times 10^{-3} \text{ \AA}$ (or 0.0286%) larger than $a_{\text{SRM}} \simeq 4.15692(1) \text{ \AA}$, respectively¹¹. The Rietveld refinements with a fixed value of a_{SRM} were conducted. The reliability factors $R_{\text{wp}}^{\text{fix},(152)}$ and $R_{\text{wp}}^{\text{fix},(92)}$ are 8.355% and 8.623%, respectively, where the superscript ‘fix’ refers to the ‘fixed’. Significantly, $R_{\text{wp}}^{\text{fix}}$ is larger than $R_{\text{wp}}^{\text{cnv}}$, implying that R_{wp} is an incomplete criterion of fit. Note that a difference between $R_{\text{wp}}^{\text{fix}}$ and $R_{\text{wp}}^{\text{cnv}}$ is not caused by the difference of the number of parameters in each refinement because R_c , which corresponds to mathematically expected R_{wp} , is $R_c^{\text{fix},(152)} = R_c^{\text{cnv},(152)} = 8.203\%$ and $R_c^{\text{fix},(92)} = R_c^{\text{cnv},(92)} = 4.090\%$, and are the same with each other independent on the number of parameters.

Figure 1a and b show the 2θ -dependence of the peak-shift $\Delta 2\theta_{\text{R}}$ computed with the following equation¹²:

$$\Delta 2\theta_{\text{R}} = Z + D_s \cos \theta + T_s \sin 2\theta, \quad (1)$$

where Z is the zero-point shift (also known as the zero error), D_s the specimen-displacement parameter and T_s the specimen-transparency parameter. Manually estimated peak-shift, $\Delta 2\theta_{\text{m}}$, is also plotted. Note that the 2θ -regions with grey background in Fig. 1 are not used in the Rietveld refinement. Clearly, $\Delta 2\theta_{\text{R}}^{\text{fix}}$ and $\Delta 2\theta_{\text{m}}$ correspond well with each other within an error bar in the analysis 2θ -region (white area). In contrast, $\Delta 2\theta_{\text{R}}^{\text{cnv}}$ differs from $\Delta 2\theta_{\text{R}}^{\text{fix}}$ and $\Delta 2\theta_{\text{m}}$ especially in the large 2θ -region.

Figure 1c and d show the 2θ -dependence of the difference, $\Delta 2\theta_{\text{dif}} \equiv \Delta 2\theta_{\text{R}}^{\text{cnv}} - \Delta 2\theta_{\text{R}}^{\text{fix}}$, which could be zero when $a = a_{\text{SRM}}$. Otherwise, the absolute value of $\Delta 2\theta_{\text{dif}}$ increases with 2θ . Moreover, $\Delta 2\theta_{\text{dif}}$ is not negligible with respect to the magnitude compared to $\Delta 2\theta_{\text{R}}^{\text{fix}}$ and $\Delta 2\theta_{\text{m}}$ (Fig. 1a and b). Note that $\Delta 2\theta_{\text{dif}}$ can be expressed by Eq. (1) with a different set of values of (Z^{cnv} , D_s^{cnv} , T_s^{cnv}) and (Z^{fix} , D_s^{fix} , T_s^{fix}). Most importantly, in the analysis 2θ -range, the 2θ -dependence of $\Delta 2\theta_{\text{dif}}$ corresponds well with that of $\Delta 2\theta_{\text{ana}}$, which is expressed as:

$$\Delta 2\theta_{\text{ana}} = 2 \left\{ \sin^{-1} \left(\frac{1}{A} \sin \theta \right) - \theta \right\}, \quad (2)$$

where A is the proportional coefficient. Here, Eq. (2) is not obtained by fitting the experimental data but is formulated by rearranging the following two Bragg’s equations and, therefore holds for any crystal system:

$$\begin{aligned} 2d \sin \frac{2\theta}{2} &= \lambda, \\ 2(Ad) \sin \frac{2\theta + \Delta 2\theta_{\text{ana}}}{2} &= \lambda. \end{aligned}$$

The coefficients $A^{\text{cnv},(152)}$ and $A^{\text{cnv},(92)}$ are $a^{\text{cnv},(152)}/a_{\text{SRM}} = 0.999911$ and $a^{\text{cnv},(92)}/a_{\text{SRM}} = 1.000286$, respectively. Equally important is that $\Delta 2\theta_{\text{m}} + \Delta 2\theta_{\text{ana}}$ as well as $\Delta 2\theta_{\text{R}}^{\text{fix}} + \Delta 2\theta_{\text{ana}}$ are in good agreement with $\Delta 2\theta_{\text{R}}^{\text{cnv}}$ in the analysis 2θ -range and enhance against $\Delta 2\theta_{\text{R}}^{\text{cnv}}$ beyond $2\theta_{\max}$ (Fig. 1e and f).

Criteria of fit. To investigate a criterion of fit in detail and study how the peak-shift affects the result, we have conducted several Rietveld refinements with a fixed value of Z . Figure 2 shows the Z - and a -dependences in the conventional criterion as well as by the criteria set in this study. The sums are carried out over all the Bragg-peaks in the analysis 2θ -range for $\Sigma |\Delta 2\theta_{\text{R}}|$ and the whole 2θ -range for $\Sigma^{\text{all}} |\Delta 2\theta_{\text{R}}|$. Note that $\Sigma |\Delta 2\theta_{\text{R}}|$ and $\Sigma^{\text{all}} |\Delta 2\theta_{\text{R}}|$ are calculated from the result after the refinement. The convergence in the refinement is judged by using R_{wp} . For $\Sigma |\Delta 2\theta_{\text{R}}|$, the number of Bragg-peaks in the sum depends on $2\theta_{\max}$, and is 24 for $2\theta_{\max} = 152^\circ$ and 13 for $2\theta_{\max} = 92^\circ$. In contrast, the number of Bragg-peaks is always 25 for $\Sigma^{\text{all}} |\Delta 2\theta_{\text{R}}|$, including a reflection with the Miller indices of 432 and 520 (lattice spacing $d \simeq 0.772 \text{ \AA}$) at $2\theta \simeq 172^\circ$ that is measureable in principle but is not observed in the data.

The conventional criterion R_{wp} shows a parabolic curve with the minimum values of 8.203% at $a^{\text{cnv},(152)} = 4.15655(1) \text{ \AA}$ and 8.610% at $a^{\text{cnv},(92)} = 4.15811(22) \text{ \AA}$ as shown in Fig. 2a and b. Importantly, the minimum of R_{wp} is not at a_{SRM} , which is a strong evident that R_{wp} itself is an insufficient criterion to obtain the true lattice parameter. Further, the range of R_{wp} for $2\theta_{\max} = 92^\circ$ is much smaller than that for $2\theta_{\max} = 152^\circ$. It suggests that for the smaller $2\theta_{\max}$, it is more difficult to distinguish the minimum R_{wp} correctly.

A potential criteria $\Sigma |\Delta 2\theta_{\text{R}}|$ shows a V-shaped curve with the minimum values at $a^{\text{sum},(152)} = 4.15684(0) \text{ \AA}$ and $a^{\text{sum},(92)} = 4.15625(2) \text{ \AA}$, where the superscript ‘sum’ refers to the ‘sum’ of the peak-shift (Fig. 2c and d). The lattice parameter a^{sum} is closer to a_{SRM} compared with a^{cnv} . The magnitude of $\Sigma |\Delta 2\theta_{\text{R}}|$ for $2\theta_{\max} = 92^\circ$ is smaller than that

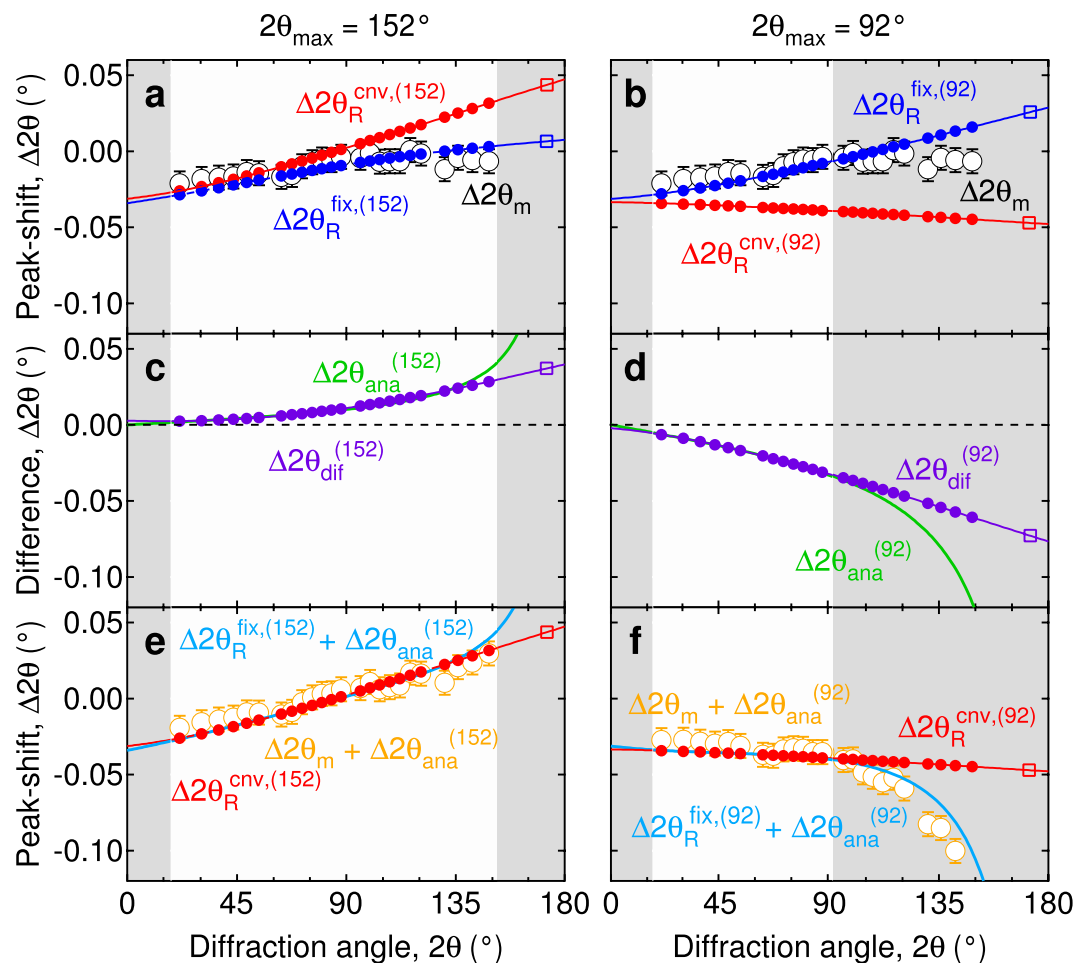


Figure 1. Diffraction angle dependence of the peak-shifts. **(a,b)** $\Delta 2\theta_R^{\text{cnv}}$, $\Delta 2\theta_R^{\text{fix}}$ and $\Delta 2\theta_m$. $\Delta 2\theta_R^{\text{cnv}}$ is obtained by conventional Rietveld refinement. Lattice parameter is fixed at a_{SRM} in Rietveld refinement for $\Delta 2\theta_R^{\text{fix}}$. $\Delta 2\theta_m$ is manually calculated by comparing 2θ -angle values of Bragg-peaks in the raw data and certification by NIST. **(c,d)** Difference $\Delta 2\theta_{\text{dif}} \equiv \Delta 2\theta_R^{\text{cnv}} - \Delta 2\theta_R^{\text{fix}}$ and analytical peak-shift $\Delta 2\theta_{\text{ana}}$. Horizontal dash line with zero intensity is drawn as visual guide. **(e,f)** Sums $\Delta 2\theta_m + \Delta 2\theta_{\text{ana}}$ and $\Delta 2\theta_R^{\text{fix}} + \Delta 2\theta_{\text{ana}}$. $\Delta 2\theta_R^{\text{cnv}}$ is again plotted for comparison. For all the panels, open squares at approximately $2\theta = 172^\circ$ are the calculated data for a reflection with the Miller indices of 432 and 520 that is not observed in the data. Note that the 2θ -regions with grey background are not used in the Rietveld refinement. Left and right panels are for $2\theta_{\text{max}} = 152^\circ$ and 92° , respectively. The error bars indicate the measurement error of the diffraction data in **(a,b,e)** and **(f)**.

for $2\theta_{\text{max}} = 152^\circ$, which is reasonable considering the number of Bragg-peaks in the sum. Our proposed criterion $\Sigma^{\text{all}}|\Delta 2\theta_R|$ shows a sharper V-shaped curve than $\Sigma|\Delta 2\theta_R|$ with the minimum values at $a^{\text{all},(152)} = 4.15686(0) \text{ \AA}$ and $a^{\text{all},(92)} = 4.15696(2) \text{ \AA}$, where the superscript ‘all’ refers to the sum of ‘all’ values of $\Delta 2\theta_R$ (Fig. 2e and f). The lattice parameter a^{all} is much closer to a_{SRM} compared with a^{cnv} and a^{sum} . With decreasing $2\theta_{\text{max}}$, the magnitude of $\Sigma^{\text{all}}|\Delta 2\theta_R|$ increases and the V-shape becomes sharper.

Figure 3a demonstrates the $2\theta_{\text{max}}$ -dependence of the lattice parameters obtained by several criteria. First, a^{cnv} , which is obtained by the conventional Rietveld method, shows a large deviation from a_{SRM} and strong dependence on $2\theta_{\text{max}}$. The maximum deviation from a_{SRM} is $>10 \times 10^{-3} \text{ \AA}$, which is in the same order as that in Hill’s report⁷. Next, a^{sum} , which is determined with the minimum of $\Sigma|\Delta 2\theta_R|$, approaches toward a_{SRM} with increasing $2\theta_{\text{max}}$. The smallest deviation from a_{SRM} is $0.08 \times 10^{-3} \text{ \AA}$ at $2\theta_{\text{max}} = 152^\circ$. Subsequently, a^{all} , which is determined by using $\Sigma^{\text{all}}|\Delta 2\theta_R|$, corresponds well with a_{SRM} even for the smaller $2\theta_{\text{max}}$. The deviation from a_{SRM} is $0.60 \times 10^{-3} \text{ \AA}$ at the most and within $0.06 \times 10^{-3} \text{ \AA}$ above $2\theta_{\text{max}} = 74^\circ$. The accuracy is improved by two or more orders of magnitude compared with that of the conventional Rietveld method.

Figure 3b shows the $2\theta_{\text{max}}$ -dependence of R_{wp} ’s. It is clear that R_{wp} increases with decreasing $2\theta_{\text{max}}$. For all $2\theta_{\text{max}}$, the values of $R_{\text{wp}}^{\text{cnv}}$ are smaller than those of $R_{\text{wp}}^{\text{all}}$ despite the fact that a^{cnv} does not correspond to a_{SRM} . The difference, $R_{\text{wp}}^{\text{all}} - R_{\text{wp}}^{\text{cnv}}$, becomes smaller with decreasing $2\theta_{\text{max}}$ and is 0.02% or less below $2\theta_{\text{max}} = 120^\circ$ as shown in Fig. 3c. It becomes zero at some $2\theta_{\text{max}}$ ’s, implying the impossibility in distinguishing the true solution exclusively by the R_{wp} -value.

Figure 3d–f show the peak-shifts determined with the minima of R_{wp} , $\Sigma|\Delta 2\theta_R|$ and $\Sigma^{\text{all}}|\Delta 2\theta_R|$. Clearly, $\Delta 2\theta_R^{\text{cnv}}$ does not reproduce $\Delta 2\theta_m$, reflecting a mismatch of the lattice parameter between a^{cnv} and a_{SRM} . Although

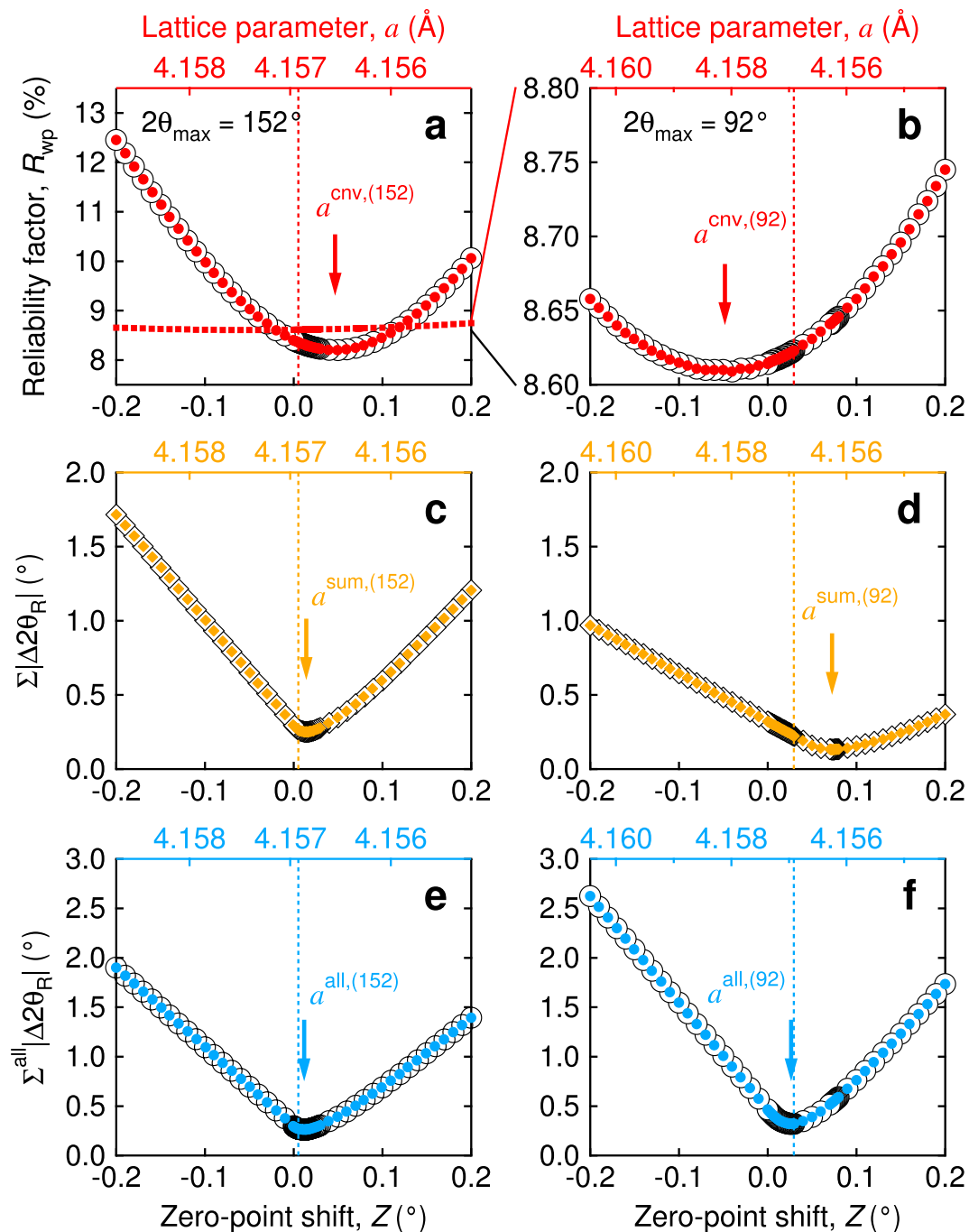


Figure 2. Conventional and candidate criteria of fit. Z - and a -dependences of (a), $R_{\text{wp}}^{\text{fix}}$ for $2\theta_{\text{max}} = 152^\circ$, (b), $R_{\text{wp}}^{\text{fix}}$ for $2\theta_{\text{max}} = 92^\circ$, (c), $\Sigma|\Delta 2\theta_{\text{R}}|$ for $2\theta_{\text{max}} = 152^\circ$, (d), $\Sigma|\Delta 2\theta_{\text{R}}|$ for $2\theta_{\text{max}} = 92^\circ$, (e), $\Sigma^{\text{all}}|\Delta 2\theta_{\text{R}}|$ for $2\theta_{\text{max}} = 152^\circ$, (f), $\Sigma^{\text{all}}|\Delta 2\theta_{\text{R}}|$ for $2\theta_{\text{max}} = 92^\circ$. Vertical dot line indicates $a = a_{\text{SRM}}$. The minimum for each criterion is shown by the arrow. (a), $R_{\text{wp}}^{\text{fix}}$ for $2\theta_{\text{max}} = 92^\circ$ is also plotted for comparison (small dots). Note that relationship between Z and a for $2\theta_{\text{max}} = 152^\circ$ (left panels) and that for $2\theta_{\text{max}} = 92^\circ$ (right panels) are not the same.

$\Delta 2\theta_{\text{R}}^{\text{sum}}$ is closer to $\Delta 2\theta_{\text{m}}$ than $\Delta 2\theta_{\text{R}}^{\text{cnv}}$, it deviates from $\Delta 2\theta_{\text{m}}$ above $2\theta_{\text{max}}$ as shown in the inset of Fig. 3e as an example. Additionally, $\Delta 2\theta_{\text{R}}^{\text{all}}$ well reproduces $\Delta 2\theta_{\text{m}}$ for the all $2\theta_{\text{max}}$ (Fig. 3f). These facts indicate that the fitting accuracy relates directly to the well reproducibility of the peak-shift.

Discussion

The present study reveals several critical findings. Firstly, the 2θ -dependence of peak-shift does not obey Eq. (1) in the calculation; instead follows the equation:

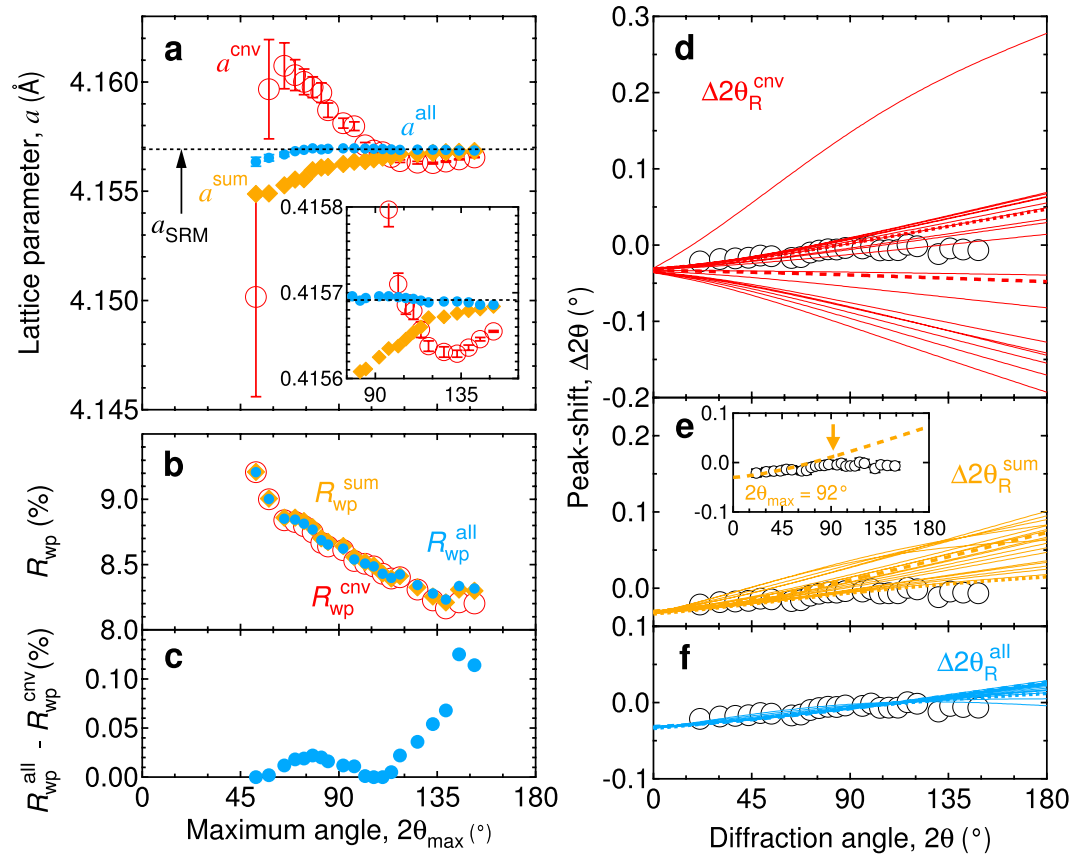


Figure 3. Comparison of obtained lattice parameters and peak-shifts. **(a)**, $2\theta_{\max}$ -dependence of lattice parameters a^{cnv} , a^{sum} and a^{all} . The error bars represent the standard error σ in the Rietveld refinement. Horizontal dot line indicates a_{SRM} . Inset: Enlarged view of a in the range of $75^\circ \leq 2\theta_{\max} \leq 165^\circ$. **(b)**, $2\theta_{\max}$ -dependence of reliability factors $R_{\text{wp}}^{\text{cnv}}$, $R_{\text{wp}}^{\text{sum}}$ and $R_{\text{wp}}^{\text{all}}$. **(c)**, $2\theta_{\max}$ -dependence of difference $R_{\text{wp}}^{\text{all}} - R_{\text{wp}}^{\text{cnv}}$. **(d,e,f)**, 2θ -dependences of peak-shifts $\Delta 2\theta_{\text{R}}^{\text{cnv}}$, $\Delta 2\theta_{\text{R}}^{\text{sum}}$ and $\Delta 2\theta_{\text{R}}^{\text{all}}$. Bold dot lines and dash lines are for $2\theta_{\max} = 152^\circ$ and 92° , respectively. **(e)**, Inset: Enlarged view of $\Delta 2\theta_{\text{R}}^{\text{sum}}$ for $2\theta_{\max} = 92^\circ$. $\Delta 2\theta_{\text{R}}^{\text{sum}}$ starts to deviate at approximately $2\theta_{\max}$ as shown by the arrow with increasing 2θ .

$$\Delta 2\theta_{\text{R}} = \zeta + \delta_{\text{s}} \cos \theta + \tau_{\text{s}} \sin 2\theta + 2 \left\{ \sin^{-1} \left(\frac{1}{A} \sin \theta \right) - \theta \right\}, \quad (3)$$

where ζ is the zero-point shift, δ_{s} the specimen-displacement parameter, τ_{s} the specimen-transparency parameter and A the proportional coefficient to lattice spacing (Fig. 1e and f). Equation (3) holds for any crystal system and can be simply rewritten as:

$$\Delta 2\theta_{\text{R}} = \Delta 2\theta_{\text{exp}} + \Delta 2\theta_{\text{ana}}, \quad (4)$$

where $\Delta 2\theta_{\text{exp}}$ is the experimental peak-shift by the geometry (includes design-geometry of instrument as well as specimen-geometry) and $\Delta 2\theta_{\text{ana}}$ is the analytical peak-shift caused by the mismatch of the lattice parameters. Notably, $\Delta 2\theta_{\text{ana}}$ exists in the calculation only when $A \neq 1$. Considering Eqs (3) and/or (4), one cannot obtain the true peak-shift when $\Delta 2\theta_{\text{ana}} \neq 0$ ($A \neq 1$). Secondly, $\Delta 2\theta_{\text{ana}}$ can be fitted very well by Eq. (1) in the analysis 2θ -range (Fig. 1c and d). The finite value of $\Delta 2\theta_{\text{ana}}$, therefore, induces a false peak-shift with irrelevant lower- R_{wp} (Fig. 2a and b). As a result, a homothetic unit-cell, which is proportional to the true one, is obtained in the conventional Rietveld method. To obtain the correct unit-cell, $\Delta 2\theta_{\text{ana}} = 0$ should be imposed. Finally, we have proposed an additional criterion, $\Sigma^{\text{all}} |\Delta 2\theta_{\text{R}}|$, which measures the fitting accuracy along the horizontal-axis of the diffraction data and is capable of preventing $\Delta 2\theta_{\text{ana}}$ from enhancing. By combining our criterion with R_{wp} , we can well reproduce the peak-shift (Fig. 3f). Consequently, we can determine the lattice parameter within the accuracy of $0.06 \times 10^{-3} \text{ \AA}$ (Fig. 3a). Incidentally, we deduce that there was no need to consider too much detail about the peak-shift in the early stage of developing the method because the angle-dispersive neutron data was used^{3,13}. Neutron has high transparency against the materials. Enough high-angle data, e.g. $2\theta_{\max} = 144^\circ$ (ref.³), with quite broad Bragg-peaks were generally obtained using an old-fashioned reactor source. As a result, the 2θ -dependence of peak-shift was approximately constant and could easily be reproduced. In fact, Rietveld applied a zero-shift parameter as the peak-shift function which is independent on 2θ (ref.³).

Our present findings possibly accelerate designing novel materials since a comparative study between the experiment and theory¹⁴ may be achieved with high-accuracy. The criterion we set in this report would be applicable for structure determination from powder diffraction^{15–17} including indexing the diffraction peaks^{18–20} and the profile decomposition^{21–23} as well as a quality management of mass production of materials in industry. Further study related to the structural parameters in the unit-cell is desirable.

In summary, an additional criterion, $\sum^{\text{all}}|\Delta 2\theta_{\text{R}}|$, to determine accurately the lattice parameter by the Rietveld method from powder diffraction data has been proposed. The refinements of the same data with different fixed-values of peak-shift parameter lead to different values of reliability factor, R_{wp} . The refined lattice parameter at the minimum R_{wp} -value is different from the correct one. The peak-shift includes the analytical $\Delta 2\theta_{\text{ana}}$ as well as the experimental $\Delta 2\theta_{\text{exp}}$ in the calculation. $\Delta 2\theta_{\text{ana}}$ must be neutralized for the analysis because it results in a false unit-cell that is proportional to the true one with the incorrect lower R_{wp} -value when $\Delta 2\theta_{\text{ana}} \neq 0$. Our criterion allows well reproducibility of the peak-shift through the highly accurate determination of lattice parameter by two or more digits lower than that compared with the conventional Rietveld method.

Methods

Powder diffraction data. Diffraction pattern used in this study was measured by Le Bail and distributed on the website²⁴. The data file with a name of “660a-2.dat” in a compressed file, x-celerator.zip, was used. The X-ray diffraction pattern for SRM 660a¹¹ was carefully collected in the range of $2\theta = 18.003^\circ - 151.995^\circ$ with a step of 0.008° by using a conventional diffractometer (Philips X’Pert, equipped with an X’Celerator detector) with Cu $K\alpha_1$ radiation. Twenty-four diffraction peaks were observed. Total measurement time was more than 17 h and the largest intensity was more than 100000 counts, realizing very good statistics and a high signal-to-background ratio. The diffraction peaks were very sharp as a full width at half-maximum (FWHM) of a diffraction peak were approximately 0.03° at the lowest angle and 0.17° at the highest angle. The peaks were fairly symmetric for the in-house data. The lattice parameter $a_{\text{SRM}} = 4.1569162(97) \text{ \AA} \approx 4.15692(1) \text{ \AA}$ at 22.5°C has been clarified by NIST¹¹.

Data analysis approach. *Rietveld refinements.* The Rietveld program RIETAN-FP²⁵ was selected to analyse the data in this study. Taking the rounding error of the program into consideration, a value of the wavelength λ (1.540593 Å for Cu $K\alpha_1$ radiation) in RIETAN-FP is the same as that used in the computation for SRM 660a¹¹ by NIST ($\lambda = 1.5405929(5) \text{ \AA}$)²⁶. Note that the other major Rietveld programs use a slightly different value for Cu $K\alpha$ radiation as default. For example, in GSAS²⁷, GSAS-II²⁸, FullProf²⁹, Z-Rietveld³⁰ and TOPAS³¹, the wavelengths of Cu $K\alpha_1$ are 1.5405 Å, 1.54051 Å, 1.54056 Å, 1.54056 Å and 1.540596 Å, respectively. The profile function of a Thompson-Cox-Hastings pseudo-Voigt function³² was used. Howard’s method³³, which is based on the multi-term Simpson’s rule integration, was employed for the profile asymmetry. Profile cut-off was 0.001%. The background function was the sixth order of Legendre polynomials.

In addition to the conventional Rietveld refinement, several sets of Rietveld refinement, with different fixed-values for the first term Z of the peak-shift, were performed. Here, the other refinement parameters were refined. This is because we have assumed that a parameter Z , which is different from the true value Z^{true} , gives R_{wp} larger than that for the true value $R_{\text{wp}}^{\text{true}}$. The range of Z between -0.2° and 0.2° was chosen considering a FWHM of a diffraction peak. For each set, a total of 157 calculation-steps were conducted to confirm that our procedure was enough to converge. Thus, our calculation is the fixed routine one that is applied to the same data set starting from different fixed Z -values for Rietveld refinement.

Peak-shift estimation. The peak-shift $\Delta 2\theta_{\text{m}} \equiv 2\theta_{\text{SRM}} - 2\theta_{\text{obs}}$ was calculated by using the raw data. The list of ideal Bragg-peak angle, $2\theta_{\text{SRM}}$, was provided in the certificate of SRM 660a¹¹. The observed diffraction angle $2\theta_{\text{obs}}$ for each reflection was chosen at the strongest intensity in the diffraction data near $2\theta_{\text{SRM}}$. The measurement error of $2\theta_{\text{obs}}$ was assumed to be the same as the step of 0.008° in the data.

Data Availability. The data that support the findings of this study are distributed by Prof. Armel Le Bail and available in the website, http://www.cristal.org/powdif/low_fwhm_and_rp.html.

References

- Rietveld, H. M. A method for including the line profiles of neutron powder diffraction peaks in the determination of crystal structures. *Acta Crystallogr.* **21**, A228 (1966).
- Rietveld, H. M. Line profiles of neutron powder-diffraction peaks for structure refinement. *Acta Crystallogr.* **22**, 151–152 (1967).
- Rietveld, H. M. A profile refinement method for nuclear and magnetic structures. *J. Appl. Crystallogr.* **2**, 65–71 (1969).
- Young, R. A. Introduction to the Rietveld method. In *The Rietveld Method*. (ed. Young, R. A.) 1–38 (Oxford Univ. Press, Oxford, United Kingdom, 1993).
- Toby, B. H. R factors in Rietveld analysis: How good is good enough? *Powder Diffr.* **21**, 67–70 (2006).
- McCusker, L. B. *et al.* Rietveld refinement guidelines. *J. Appl. Crystallogr.* **32**, 36–50 (1999).
- Hill, R. J. Rietveld Refinement round robin. I. Analysis of standard X-ray and neutron data for PbSO_4 . *J. Appl. Crystallogr.* **25**, 589–610 (1992).
- Young, R. A., Prince, E. & Sparks, R. A. Suggested guidelines for the publication of Rietveld analyses and pattern decomposition studies. *J. Appl. Crystallogr.* **15**, 357–359 (1982).
- Fei, Y. Thermal Expansion. In *Mineral Physics and Crystallography: A Handbook of Physical Constants*. (ed. Ahrens, T. J.) 29–44 (American Geophysical Union, Washington, D. C., 1995).
- Miyake, M., Minato, I., Morikawa, H. & Iwai, S. Crystal structures and sulphate force constants of barite, celestite, and anglesite. *Am. Mineral.* **63**, 506–510 (1978).
- SRM 660a. *Lanthanum Hexaboride Powder Line Position and Line Shape Standard for Powder Diffraction*. National Institute of Standards and Technology, U.S. Department of Commerce: Gaithersburg, MD, USA (2000).
- Parrish, W. & Langford, J. I. *International Tables for Crystallography. C: Mathematical, Physical and Chemical Tables* 3rd ed. (ed. Prince, E.) 42–79 (Kluwer Academic Publishers, Dordrecht, Netherlands, 2006).
- Cheetham, A. K. & Goodwin, A. L. Crystallography with powders. *Nat. Mater.* **13**, 760–762 (2014).

14. Woodley, S. M. & Catlow, A. R. Crystal structure prediction from first principles. *Nat. Mater.* **7**, 937–946 (2008).
15. David, W. I. F., Shankland, K., McCusker, L. B. & Baerlocher, C. (eds) *Structure Determination from Powder Diffraction Data*. (Oxford Univ. Press, Oxford, United Kingdom, 2002).
16. David, W. I. F. & Shankland, K. Structure determination from powder diffraction data. *Acta Crystallogr.* **A64**, 52–64 (2008).
17. Pecharsky, V. K. Solving Crystal Structure from Powder Diffraction Data. In *Fundamentals of Powder Diffraction and Structural Characterization of Materials*. 2nd ed. (eds Pecharsky, V. K. & Zavalij, P. Y.) 497–545 (Springer, New York, 2009).
18. Visser, J. W. A Fully automatic program for finding the unit cell from powder data. *J. Appl. Crystallogr.* **2**, 89–95 (1969).
19. Werner, P.-E., Eriksson, L. & Westdahl, M. TREOR, a semi-exhaustive trial-and-error powder indexing program for all symmetries. *J. Appl. Crystallogr.* **18**, 367–370 (1985).
20. Boulif, A. & Louër, D. Indexing of powder diffraction patterns for low-symmetry lattices by the successive dichotomy method. *J. Appl. Crystallogr.* **24**, 987–993 (1991).
21. Pawley, G. S. Unit-cell refinement from powder diffraction scans. *J. Appl. Crystallogr.* **14**, 357–361 (1981).
22. Le Bail, A., Duroy, H. & Fourquet, J. L. Ab-initio structure determination of LiSbWO_6 by X-ray powder diffraction. *Mat. Res. Bull.* **23**, 447–452 (1988).
23. Le Bail, A. Whole powder pattern decomposition methods and applications: A retrospection. *Powder Diffr.* **20**, 316–326 (2005).
24. Le Bail, A. Summary on the Subject 'Low FWHM and Rp'. at http://www.cristal.org/powdif/low_fwhm_and_rp.html (1994).
25. Izumi, F. & Momma, K. Three-dimensional visualization in powder diffraction. *Solid State Phenom.* **130**, 15–20 (2007).
26. Hölzer, G. *et al.* $K\alpha_{1,2}$ and $K\beta_{1,3}$ x-ray emission lines of the 3d transition metals. *Phys. Rev. A* **56**, 4554–4568 (1997).
27. Larson, A. C. & Von Dreele, R. B. *General structure analysis system (GSAS)*. Los Alamos Natl. Lab. Rep. LAUR 86–748 (2004).
28. Toby, B. H. & Von Dreele, R. B. GSAS-II: the genesis of a modern open-source all purpose crystallography software package. *J. Appl. Crystallogr.* **46**, 544–549 (2013).
29. Rodríguez-Carvajal, J. Recent advances in magnetic structure determination by neutron powder diffraction. *Physica B* **192**, 55–69 (1993).
30. Oishi-Tomiyasu, R. *et al.* Application of matrix decomposition algorithms for singular matrices to Pawley method in Z-Rietveld. *J. Appl. Crystallogr.* **45**, 299–308 (2012).
31. Coelho, A. A. A bond constrained conjugate gradient solution method as applied to crystallographic refinement problem. *J. Appl. Crystallogr.* **38**, 455–461 (2005).
32. Thompson, P., Cox, D. E. & Hastings, J. B. Rietveld refinement of Debye–Scherrer synchrotron X-ray data from Al_2O_3 . *J. Appl. Crystallogr.* **20**, 79–83 (1987).
33. Howard, C. J. The approximation of asymmetric neutron powder diffraction peaks by sums of Gaussians. *J. Appl. Crystallogr.* **15**, 615–620 (1982).

Acknowledgements

The authors thank Armel Le Bail for kindly allowing us to use his high-quality data. We are grateful to Biswajit Paik for critically reading an early version of the manuscript.

Author Contributions

M.T. planned and overseen this research. Data analyses were performed by M.T. and cross-checked the results by J.K. All authors contributed to the manuscript preparation.

Additional Information

Competing Interests: M.T.'s institution is currently applying for patents in Japan (JP appl. No. 2017-110500 filed on 2 June 2017) related to this work. J.K. declares no competing financial interests.

Publisher's note: Springer Nature remains neutral with regard to jurisdictional claims in published maps and institutional affiliations.



Open Access This article is licensed under a Creative Commons Attribution 4.0 International License, which permits use, sharing, adaptation, distribution and reproduction in any medium or format, as long as you give appropriate credit to the original author(s) and the source, provide a link to the Creative Commons license, and indicate if changes were made. The images or other third party material in this article are included in the article's Creative Commons license, unless indicated otherwise in a credit line to the material. If material is not included in the article's Creative Commons license and your intended use is not permitted by statutory regulation or exceeds the permitted use, you will need to obtain permission directly from the copyright holder. To view a copy of this license, visit <http://creativecommons.org/licenses/by/4.0/>.

© The Author(s) 2017